

# Neuro-Oncology Advances

## Pharmacokinetic Properties of the Temozolomide Perillyl Alcohol Conjugate (NEO212) in Mice --Manuscript Draft--

<b>Manuscript Number:</b>	NOA-D-20-00118R2
<b>Full Title:</b>	Pharmacokinetic Properties of the Temozolomide Perillyl Alcohol Conjugate (NEO212) in Mice
<b>Short Title:</b>	Pharmacokinetics of NEO212
<b>Article Type:</b>	Basic and Translational Investigations
<b>Keywords:</b>	glioblastoma, pharmacokinetic, temozolomide, NEO212, HPLC
<b>Corresponding Author:</b>	Thomas C Chen, M.D., PhD Keck School of Medicine Los Angeles, CA UNITED STATES
<b>Corresponding Author Secondary Information:</b>	
<b>Corresponding Author's Institution:</b>	Keck School of Medicine
<b>Corresponding Author's Secondary Institution:</b>	
<b>First Author:</b>	Thomas C C Chen, M.D., PhD
<b>First Author Secondary Information:</b>	
<b>Order of Authors:</b>	Thomas C C Chen, M.D., PhD Hee-Yeon Cho Steve Swenson Thu Zan Thein Weijun Wang Neloni R. Wijeratne Nagore I. Marin-Ramos Jonathan E. Katz Florence M. Hofman Axel H. Schönthal Thomas C. Chen
<b>Order of Authors Secondary Information:</b>	
<b>Manuscript Region of Origin:</b>	UNITED STATES
<b>Abstract:</b>	NEO212 is a novel small-molecule anticancer agent that was generated by covalent conjugation of the natural monoterpene perillyl alcohol (POH) to the alkylating agent temozolomide (TMZ). It is undergoing preclinical development as a therapeutic for brain-localized malignancies. The aim of this study was to characterize metabolism and pharmacokinetic (PK) properties of NEO212 in preclinical models. We used mass spectrometry and modified high-performance liquid chromatography (HPLC) to identify and quantitate NEO212 and its metabolites in cultured glioblastoma cells, in mouse serum, brain and excreta after oral gavage. Our methods allowed identification and quantitation of NEO212, POH, TMZ, as well as primary metabolites 5-aminoimidazole-4-carboxamide (AIC) and perillic acid (PA). Intracellular concentrations of TMZ were greater after treatment of U251 cells with NEO212 than after treatment with TMZ. The half-life of NEO212 in mouse serum was 94 minutes. In mice harboring syngeneic GL261 brain tumors, the amount of NEO212 was greater in the tumor-bearing

	hemisphere than in the contralateral normal hemisphere. The brain:serum ratio of NEO212 was greater than that of TMZ. Excretion of unaltered NEO212 was through feces, whereas its AIC metabolite was excreted via urine. NEO212 preferentially concentrates in brain tumor tissue over normal brain tissue, and compared to TMZ has a higher brain:serum ratio, altogether revealing favorable features to encourage its further development as a brain-targeted therapeutic. Its breakdown into well-characterized, long-lived metabolites, in particular AIC and PA, will provide useful equivalents for PK studies during further drug development and clinical trials with NEO212.
<b>Suggested Reviewers:</b>	Nicholas Butowski nicholas.butowski@ucsf.edu
<b>Opposed Reviewers:</b>	
<b>Additional Information:</b>	
<b>Question</b>	<b>Response</b>
KEY POINTS: Please enter two to three Key Points that summarize the most important findings of your manuscript. Each of these should be no longer than 85 characters and spaces (all together 260 characters). These points may be used to highlight your article on social media.	<ol style="list-style-type: none"> <li>1. We developed HPLC methods to quantify NEO212 and its metabolites.</li> <li>2. NEO212 concentrates in tumor tissue over normal tissue and has a higher brain to serum ratio than TMZ.</li> <li>3. PK properties of NEO212 support further development toward clinical testing.</li> </ol>



28 **Funding**

29 This study was supported by the Sharyl and Oscar Garza Fund (to T.C.C.), Michael Kriegel  
30 Foundation (to T.C.C.), Sounder Foundation (to T.C.C.), and by NeOnc Technologies, Inc. (to  
31 H.Y.C., S.S.), NIH 1R41 CA192419-01A1 (to T.C.C., F.M.H)

32

33 **Conflict of interest**

34 Thomas C. Chen is an officer and shareholder of NeOnc Technologies, Inc. (Los Angeles, CA).  
35 The other authors declare that they have no conflict of interests.

36

37 **Authorship**

38 H.-Y.C. designed and performed experiments, contributed to data collection and analysis, and  
39 drafted the manuscript. S.S. performed experiments and drafted the manuscript. T.Z.T.  
40 performed experiments and reviewed the manuscript. W.W. performed experiments. N.R.W.  
41 performed experiments. N.I.M.-R. contributed to study design, data analysis, and reviewed the  
42 manuscript. J.E.K. performed data analysis and interpretation of results. A.H.S. contributed to  
43 study design and data analysis, and finalized the manuscript. F.M.H. contributed to study design  
44 and data analysis. T.C.C. conceived of the study, acquired funding, contributed to study design,  
45 data analysis and supervision, and reviewed the manuscript. All authors approved the final  
46 version of the manuscript.

47

48

49 **Abstract**

50

51 **Background.** NEO212 is a novel small-molecule anticancer agent that was generated by  
52 covalent conjugation of the natural monoterpene perillyl alcohol (POH) to the alkylating agent  
53 temozolomide (TMZ). It is undergoing preclinical development as a therapeutic for brain-  
54 localized malignancies. The aim of this study was to characterize metabolism and  
55 pharmacokinetic (PK) properties of NEO212 in preclinical models.

56

57 **Methods.** We used mass spectrometry (MS) and modified high-performance liquid  
58 chromatography (HPLC) to identify and quantitate NEO212 and its metabolites in cultured  
59 glioblastoma cells, in mouse plasma, brain and excreta after oral gavage.

60

61 **Results.** Our methods allowed identification and quantitation of NEO212, POH, TMZ, as well as  
62 primary metabolites 5-aminoimidazole-4-carboxamide (AIC) and perillic acid (PA). Intracellular  
63 concentrations of TMZ were greater after treatment of U251TR cells with NEO212 than after  
64 treatment with TMZ. The half-life of NEO212 in mouse plasma was 94 minutes. In mice  
65 harboring syngeneic GL261 brain tumors, the amount of NEO212 was greater in the tumor-  
66 bearing hemisphere than in the contralateral normal hemisphere. The brain:plasma ratio of  
67 NEO212 was greater than that of TMZ. Excretion of unaltered NEO212 was through feces,  
68 whereas its AIC metabolite was excreted via urine.

69

70 **Conclusions.** NEO212 preferentially concentrates in brain tumor tissue over normal brain  
71 tissue, and compared to TMZ has a higher brain:plasma ratio, altogether revealing favorable  
72 features to encourage its further development as a brain-targeted therapeutic. Its breakdown  
73 into well-characterized, long-lived metabolites, in particular AIC and PA, will provide useful  
74 equivalents for PK studies during further drug development and clinical trials with NEO212.

75

76

77 **Key words:** glioblastoma, pharmacokinetic, temozolomide, NEO212, HPLC

78

79

80 **Key points**

81

82 1. We developed HPLC methods that allowed identification and quantitation of NEO212 and its  
83 metabolites in cells, plasma and tissue.

84 2. NEO212 preferentially concentrates in brain tumor tissue over normal brain tissue and has a  
85 higher brain:plasma ratio than TMZ.

86 3. PK properties of NEO212 are favorable and support further development toward clinical  
87 testing.

88

89

90 **Importance of the study**

91

92 NEO212 is the conjugate of temozolomide (TMZ) to perillyl alcohol (POH). Our previous studies  
93 had demonstrated its superior efficacy compared to TMZ in a variety of tumor cell types,  
94 including MGMT-positive and other TMZ-resistant variants. This current report is significant  
95 because it is the first time that the direct mechanism, potency, brain penetration, and  
96 metabolism of NEO212 have been directly measured and compared to TMZ. NEO212 stabilizes  
97 the prodrug TMZ, and allows better BBB penetrance (up to 3x), greater cellular uptake and  
98 increased potency (up to 10x). Its mechanism of action remains based on DNA alkylation, with  
99 AIC as its main breakdown product, and myelodysplasia as its primary toxicity. Our goal is to  
100 get NEO212 to the clinic to be used in metastatic and primary brain cancers.

101

102

**103 Introduction**

104

105 NEO212 is a novel small-molecule anticancer agent currently undergoing preclinical  
106 development. It was generated by covalent conjugation of perillyl alcohol (POH) to the alkylating  
107 agent temozolomide (TMZ). Oral TMZ is the current chemotherapeutic standard of care for the  
108 treatment of patients with newly diagnosed glioblastoma (GB), where it is administered  
109 concomitantly with radiotherapy and subsequently as monotherapy during the adjuvant phase <sup>1,2</sup>.  
110 TMZ acts as a pro-drug; it undergoes spontaneous hydrolysis at physiological pH into its active  
111 metabolite, 5-(3-methyl triazen-1-yl) imidazole-4-carboxamide (MTIC) <sup>3</sup>. This product is then  
112 rapidly degraded into a methyldiazonium ion, representing the reactive species that methylates  
113 the DNA, and the inactive metabolite 5-aminoimidazole-4-carboxamide (AIC), which is stable in  
114 plasma for >24 h and is excreted through the kidneys <sup>3,4</sup>. The interaction of the methyldiazonium  
115 ion with DNA yields a variety of alkylated bases, of which O<sup>6</sup>-methylguanine (O<sup>6</sup>MeG) is  
116 considered the most cytotoxic lesion <sup>5</sup>.

117

118 Several resistance mechanisms have been recognized that can protect cells from the cytotoxic  
119 impact of TMZ treatment. Foremost is overexpression of O<sup>6</sup>-methylguanine DNA  
120 methyltransferase (MGMT), a DNA repair enzyme that specifically removes the added methyl  
121 group from O<sup>6</sup>MeG, thereby eliminating the prime cytotoxic lesion set by TMZ <sup>5</sup>. Separately, lack  
122 of an efficient DNA mismatch repair (MMR) system can provide TMZ resistance, because  
123 O<sup>6</sup>MeG lesions require functional MMR in order to trigger the double-strand breaks that lead to  
124 apoptosis <sup>6</sup>. Other DNA lesions, in particular alkylation of N-purines by TMZ, are generally  
125 restored by base-excision repair (BER), and therefore increased activity of the BER system can  
126 provide an additional layer of resistance to TMZ. Based on this variety of molecular defenses  
127 against TMZ, it is not surprising that in clinical practice most GB patients experience  
128 recurrences, where the tumor has become unresponsive to further treatment with TMZ <sup>3,7</sup>. Better  
129 treatments are urgently needed, and to address this medical need we have been developing  
130 NEO212, which might be able to overcome some of the shortcomings of TMZ <sup>8,9</sup>.

131

132 In NEO212, TMZ has been conjugated to POH, a naturally occurring monoterpene and  
133 metabolic product of limonene. It is commonly found in the essential oils of several plants and  
134 fruits, such as peppermint, spearmint, cherries and celery seeds. POH has long been reported  
135 to have anticancer effects in vitro and in vivo <sup>10</sup>. While initially it was characterized as an  
136 inhibitor of Ras oncoprotein, additional pleiotropic effects were described, including inhibition of

137 telomerase activity and aggravation of endoplasmic reticulum stress <sup>11,12</sup>, altogether exerting  
138 these effects primarily in cancer cells where these components already are overly active. The  
139 cancer therapeutic activity of POH was further investigated in several phase I/II clinical trials,  
140 where it was administered orally in rather large quantities <sup>10</sup>. However, the documented  
141 anticancer activity was unimpressive, and patients found the continuous daily regimen hard to  
142 tolerate. As a result, oral POH did not enter clinical practice. As an alternative, an intranasal  
143 formulation of POH was developed, and currently ongoing clinical trials are revealing well-  
144 tolerated, promising activity of this approach in patients with recurrent GB <sup>13,14</sup>. The two main  
145 metabolites of POH in mammals were identified as perillic acid (PA) and dihydroperillic acid  
146 (DHPA) <sup>15</sup> while the parental molecule, POH itself, was difficult to detect, presumably due to its  
147 very short biological half-life <sup>15-17</sup>.

148

149 In conjugating POH with TMZ, we desired to create a molecule with beneficial features  
150 contributed by both of its components, i.e., alkylation function and pleiotropic impairment of  
151 cancer cell-specific hallmarks. In addition, our *in silico* analysis of NEO212 predicted effective  
152 penetration of the blood-brain barrier (BBB) and higher brain-targeted activity as compared to  
153 TMZ <sup>18</sup>. Thus, results from computer modeling made NEO212 particularly attractive for  
154 development as a brain cancer agent.

155

156 NEO212 has revealed robust cancer therapeutic activity in a wide variety of *in vitro* and *in vivo*  
157 tumor models. In mouse tumor models, NEO212 displayed intracranial activity not only against  
158 GB <sup>9,19</sup>, but also against brain-metastatic breast cancer xenografts <sup>18</sup>. Beside intracranial tumors,  
159 NEO212 was also effective against peripheral cancers, such as subcutaneous melanoma <sup>20</sup>,  
160 nasopharyngeal carcinoma <sup>21,22</sup>, ovarian carcinoma <sup>23</sup>, lung cancer <sup>24-26</sup>, and cutaneous T-cell  
161 lymphoma <sup>27</sup>. In addition, NEO212 exerted activity even against TMZ-resistant cells, irrespective  
162 of the underlying resistance mechanism. At the same time, treatment was well tolerated by the  
163 tumor-bearing animals and no signs of toxicity could be detected. Intriguingly, whenever  
164 NEO212 was compared side-by-side to treatments with TMZ or POH individually, the  
165 conjugated compound consistently displayed significantly greater anticancer activity.  
166 Combination treatments with mixtures of TMZ with POH were unable to mimic the superior  
167 effects of NEO212, demonstrating that the potency of the conjugated compound is greater than  
168 the sum of its parts <sup>8,9,19,20</sup>.

169

170 Although NEO212 has been extensively studied at the preclinical level, no plasma or brain PK  
171 data are available. As well, its *in silico*-predicted efficient BBB penetration has not been  
172 confirmed experimentally, nor has it been established whether treatment with NEO212 would  
173 indeed generate the predicted metabolites *in vivo*. This latter point is of particular relevance,  
174 because knowledge of metabolites and the availability of respective assays to measure them  
175 are needed in preparation for clinical studies of NEO212. In the following, we are presenting the  
176 analytical identification and PK measurement of NEO212 and its key metabolites in plasma and  
177 brain of mice.

178

## 179 **Materials and Methods**

180

### 181 **Cell lines**

182 The human glioma cell lines U251, LN229 and T98G were purchased from the American Tissue  
183 Culture Collection (ATCC, Manassas, VA). The U251-derived TMZ-resistant (TR) cell line was  
184 developed in this laboratory<sup>9</sup> and the mouse glioma cell line GL261 was provided by Dr. Linda  
185 M. Liau (University of California Los Angeles). Chemoresistant glioma cancer stem cells USC02  
186 were isolated from a patient with glioblastoma as described previously<sup>19</sup>. Cell culture conditions  
187 were as described elsewhere<sup>28</sup> and further details are provided in Supplementary Materials.

188

### 189 **Pharmacological agents**

190 NEO212 was synthesized by Norac Pharma (Azusa, CA) under cGMP conditions as a  
191 crystalline powder and was kindly provided by NeOnc Technologies, Inc. (Los Angeles, CA). A  
192 stock solution (1M in DMSO) was further diluted with a 50:50 mixture (vol:vol) of glycerol and  
193 ethanol before being administered to animals by oral gavage. For cell culture treatments, the  
194 stock solution was diluted with cell culture medium. TMZ was purchased from Sigma Aldrich (St.  
195 Louis, MO) and dissolved in DMSO to a concentration of 50mM before administered to animals  
196 or cell culture. DMSO, glycerol and ethanol were purchased from Sigma Aldrich.

197

### 198 **Xenografts**

199 All animal protocols were approved by the Institutional Animal Care and Use Committee (IACUC)  
200 of USC, and all rules and regulations were followed during experimentation. Intracranial  
201 implantation of mouse glioma cells (GL261) was performed as previously described<sup>28</sup>. At 12  
202 days post implantation, animals were randomly separated into different treatment groups with 3  
203 animals in each group. The drugs were administered by oral gavage for a one-time treatment.

204 At different time points thereafter, animals were euthanized. Blood was collected immediately,  
205 followed by perfusion and harvest of brains. Brains were then separated into their right and left  
206 hemispheres, with and without tumor tissue, respectively. All the samples were processed for  
207 HPLC analysis.

208

#### 209 **NEO212 and AIC detection in urine and feces**

210 Using a metabolic cage, the excrements from 3 mice were collected over three separate time  
211 periods, from 0-1 hour, 0-4 hours and 0-24 hours. Solid material was homogenized in PBS and  
212 filtered through a 0.22  $\mu\text{m}$  filter with the resultant filtrate again filtered through a 4k molecular  
213 weight cutoff filter. 100  $\mu\text{l}$  of filtrate was then placed in 200  $\mu\text{l}$  acetonitrile for NEO212 analysis  
214 and 100  $\mu\text{l}$  of filtrate was mixed with 200  $\mu\text{l}$  5% acetonitrile in water for AIC analysis. Urine was  
215 treated in a similar fashion without homogenization, but using the same filter units. The volume  
216 of the samples was standardized with water.

217

#### 218 **Half-life study of NEO212 and TMZ in mice**

219 Female 6-8-week-old C57BL/6 mice, weighing approximately 30 grams, were obtained from  
220 Charles River Laboratories. The mice were grouped as follows: (1) no treatment, (2) vehicle  
221 treated, (3) NEO212 treated (50 mg/kg), and (4) TMZ treated (50 mg/kg). The drugs were  
222 administered by oral gavage for a one-time treatment, and blood samples were collected at  
223 different time points thereafter: 15, 60, 120, and 240 minutes (n=3). The half-life was  
224 determined by a non-linear fit of the concentrations over time using one-phase decay.

225

#### 226 **Analytical procedures for NEO212 and its metabolites**

227 See Supplementary Materials for detailed methods of mass spectrometry (MS) and high-  
228 performance liquid chromatography (HPLC).

229

#### 230 **Statistical analysis**

231 The calculation of plasma pharmacokinetic parameters was carried out using a non-linear  
232 regression analysis from the point of maximum observed concentration. The concentrations for  
233 each sample were calculated from the AUC values for the AIC peaks detected. AUC values  
234 were calculated using a standard curve of NEO212 and AIC, which was obtained by spiking  
235 samples of tissue, substances, or fluids with these agents. The p-values were determined by a  
236 two-way ANOVA analysis of the data and  $p < 0.05$  was considered significant.

237

## 238 Results

239

### 240 The chemical structure and breakdown products of NEO212

241 NEO212 was synthesized by covalently conjugating TMZ to POH via carbamate bonding. The  
242 resultant product was authenticated by  $^1\text{H}$  and  $^{13}\text{C}$  nuclear magnetic resonance (NMR)  
243 spectroscopy and by comparison to specified reference standards, and verified to be 99.6%  
244 pure. NEO212's CAS number is 1361198-79-9, with 372.379 molecular weight and a molecular  
245 formula of  $\text{C}_{17}\text{H}_{20}\text{N}_6\text{O}_4$ . It is an off-white to light yellow to light brown crystalline solid that readily  
246 dissolves in organic solvents. Based on the known metabolites of TMZ and POH, which have  
247 been extensively documented, we predicted that NEO212 would break down in a biological  
248 system as outlined in **Figure 1A**. The carbamate bridge between TMZ and POH would be  
249 amenable to hydrolysis by esterases, presumably yielding both of the individual partner  
250 molecules, TMZ and POH, and possibly slightly modified versions thereof, depending on the  
251 exact cleavage site. TMZ is known to convert to short-lived MTIC, which is followed by  
252 degradation into long-lived AIC plus the DNA alkylating methyldiazonium ion <sup>3,4</sup>. POH is known  
253 to be metabolized to short-lived perillyl aldehyde (PALD), followed by conversion to more stable  
254 PA <sup>29,30</sup>.

255

256 We employed a modified MS approach to begin our investigation of NEO212 breakdown. Using  
257 this method, we were able to identify NEO212 (**Figure 1B**). In addition, we could also document  
258 the presence of TMZ and POH, confirming that both individual partner molecules could be  
259 derived from the conjugated parent molecule. The mass spectrogram also showed a peak at  
260 138 (identified as AIC), a peak at 390 (identified as NEO212- $\text{NH}_4^+$ , a reaction product with the  
261 solvent), and a peak at 239 (TMZ-carboxylic acid). To achieve faster and routine quantification  
262 of these molecules, especially in view of our preclinical and future clinical pharmacokinetic  
263 demands, we developed modified HPLC-based analytical approaches. As shown in  
264 **Supplementary Figure S1**, these procedures were able to readily detect and quantitate  
265 NEO212, TMZ, POH, and importantly AIC and PA, which are stable metabolites and therefore  
266 suitable as indirect readouts of overall drug exposure in a biological system. In all, both MS and  
267 HPLC demonstrated that NEO212 could yield its two main partner molecules and their  
268 metabolites, enabling us to apply these validated methods to biological systems, i.e., cultured  
269 cells and mouse-derived tissues.

270

### 271 Cellular uptake of NEO212

272 An intriguing observation in all our prior studies was the consistently documented ability of  
273 NEO212 to demonstrate high anticancer potency than TMZ, both *in vitro* and *in vivo*. To  
274 investigate our hypothesis that differential drug uptake might be involved, we treated human  
275 U251TR glioblastoma cells with NEO212 or the same concentration of TMZ, followed by  
276 analysis of intracellular concentrations of TMZ and AIC over time. As shown in **Figure 2A and**  
277 **2B**, the amounts of TMZ and AIC inside cells were substantially greater after treatment with  
278 NEO212 (>10-fold higher) than after treatment with TMZ. All differences were statistically  
279 significant. The intracellular presence of TMZ could be verified up to 120 minutes after start of  
280 drug treatment, but became undetectable at 240 minutes (**Figure 2A**). In comparison, the  
281 intracellular amount of AIC remained high and easily detectable up to 240 minutes (**Figure 2B**),  
282 consistent with this metabolite's known greater stability as compared to TMZ. Nonetheless at all  
283 time points, exposure of cells to NEO212 resulted in much more TMZ and AIC inside cells than  
284 exposure to equal concentrations of TMZ, indicating that uptake of NEO212 is more efficient  
285 than uptake of TMZ. As AIC may represent an indirect readout for production of the active DNA  
286 alkylating species, i.e., the diazonium ion, higher levels of AIC in NEO212-treated cells over  
287 TMZ-treated cells provide a reasonable rationale to explain NEO212's greater anticancer impact.  
288 We compared the cytotoxic difference between NEO212 and TMZ in U251TR cells, which  
289 clearly correlates with their intracellular presence, i.e., higher intracellular levels of NEO212  
290 (and metabolites) correlate with higher cytotoxic impact in these tumor cells (**Figure 2C**). We  
291 also used different glioma cell lines (LN229 and T98G) to monitor TMZ and AIC level after TMZ  
292 or NEO212 treatments. As shown in **Supplementary Figure S2A and S2B**, exposure of cells to  
293 NEO212 consistently resulted in much more TMZ and AIC inside cells than exposure to equal  
294 concentrations of TMZ, indicating that uptake of NEO212 was more efficient than uptake of TMZ  
295 in all the cell lines we tested. Additionally, we used chemoresistant glioma cancer stem cells  
296 (GSCs) to compare cellular uptake of NEO212 and TMZ in relation to these drug's cytotoxic  
297 impact. Consistent with the above findings with established cell lines, cellular uptake of NEO212  
298 was substantially greater than uptake of TMZ in GSCs; correspondingly, while these cells were  
299 resistant to TMZ, NEO212 was able to exert pronounced cytotoxic impact (**Supplementary**  
300 **Figure S3**).

301

### 302 **Half-life of NEO212 in mouse plasma**

303 We next determined pharmacokinetic properties of NEO212 in mice. To measure the half-life of  
304 NEO212 in plasma, a single dose of 50 mg/kg NEO212 was administered by oral gavage,  
305 followed by blood collections at different time points thereafter. Plasma measurements revealed

306 peak NEO212 concentrations at 15 minutes after dosing, which represented the earliest  
307 measured time point (**Figure 3A left**). Subsequently, NEO212 concentrations decreased over  
308 the following 2 hours and became undetectable at 24 hours (24 hour time point not shown). The  
309 calculated half-life was 94 minutes. NEO212 plasma concentrations after subcutaneous  
310 administration of NEO212 (50 mg/kg) was also measured (**Figure 3A right**). The results  
311 demonstrated that NEO212 reached its peak concentration in the plasma in 30 minutes and  
312 decreased with time and no NEO212 was detected after 24 hour. The results were similar under  
313 both conditions, indicating comparable NEO212 half-life. We next studied the plasma kinetics of  
314 AIC, after administration of NEO212 and TMZ. Mice received a single dose of 50 mg/kg  
315 NEO212 or TMZ by oral gavage, followed by blood collections at different time points thereafter.  
316 **Figure 3B** shows that peak AIC concentrations were reached within 15 minutes of NEO212  
317 dosing, followed by a slow decrease over time and significant amounts of AIC still detectable  
318 after 240 minutes. The calculated half-life of AIC was 90 minutes. AIC levels after dosing of  
319 mice with TMZ followed a similar pattern, although at slightly lower overall levels and shorter  
320 half-life of 80 minutes. In all, these measurements revealed somewhat greater *in vivo* stability of  
321 NEO212 and higher levels of AIC, as compared to TMZ, and therefore provided additional  
322 aspects that might underlie NEO212's superior anticancer potency.

323

### 324 **Neuropharmacokinetics of NEO212**

325 Our prior *in silico* analysis predicted that NEO212 would be able to cross the BBB more  
326 effectively than TMZ<sup>18</sup>. Studies with tumor-bearing mice showed that NEO212 indeed was more  
327 active than TMZ against brain-localized disease<sup>8</sup>, further supporting the initial prediction. To  
328 quantitate this effect, we measured brain:plasma ratios of both agents after treatment of mice  
329 with either NEO212 or TMZ. As shown in **Figure 3C**, the brain:plasma ratio of NEO212 was 3-  
330 times greater than that of TMZ, which was in agreement with our earlier studies and validated  
331 yet another desirable attribute of NEO212, especially in view of applications in glioblastoma  
332 therapy.

333

334 We next investigated whether the uptake of NEO212 would be different in a normal brain as  
335 compared to one harboring a brain tumor. C57BL/6 mice, with or without intracranially implanted  
336 syngeneic GL261 mouse glioma cells, received a single dose of oral NEO212. Their brains  
337 were collected at different times thereafter and analyzed for NEO212 and AIC. The results show  
338 that the concentrations of both molecules were consistently about 2-3-times higher in tumor-  
339 bearing brains than in normal brains. The highest levels of NEO212 were detected at 15

340 minutes after drug treatment, with a subsequent slow decline over the following 2 hours (**Figure**  
341 **4A**). In comparison, AIC levels displayed the inverse kinetic, i.e., the metabolite continuously  
342 increased during the 2-hour period of measurement (**Figure 4B**). The significantly greater  
343 presence of these molecules in tumor-bearing brains, in particular 3-times more AIC (the  
344 indirect indicator of DNA alkylating discharge), would be considered a benefit for future  
345 therapeutic purposes.

346  
347 We also investigated whether the above observed differential brain tumor uptake of NEO212  
348 would be reflected in differential brain:plasma ratios at the same time points. For this purpose,  
349 we compared NEO212 concentrations from tumor-bearing brains and normal brains to those  
350 measured in the plasma obtained from the same animals. As shown in **Figure 4C**, the brain:  
351 plasma ratio was consistently 2-3-fold higher in brains with tumors, further confirming that  
352 NEO212 preferentially enters brain tumors over normal brain tissue.

353  
354 We also measured POH and PA concentrations in the same samples described above. **Figure**  
355 **4D** shows that the POH concentrations were about 2-3-times higher in tumor-bearing brains  
356 than in normal brains. The highest POH concentration was reached in 15 minutes. The POH  
357 metabolite, PA levels however showed inverse kinetics like AIC and PA continuously increased  
358 and reached its highest concentrations after 2 hours (**Figure 4E**). The significantly greater  
359 presence of these molecules in tumor-bearing brains, in particular 3-times more AIC (the  
360 indirect indicator of DNA alkylating discharge), bodes well for future therapeutic purposes.

#### 361 362 **Excretion of NEO212**

363 The excretion kinetics of NEO212 and AIC were determined by evaluating feces and urine  
364 collected during specific time periods after oral delivery of a single dose of NEO212 to mice.  
365 **Figure 5A** shows that NEO212 was excreted preferentially in feces rather than urine, with the  
366 majority of it being excreted after the first 4 hours post-dosing. **Figure 5B** shows that AIC was  
367 present in the urine and barely detectable in feces, with the majority of it being excreted within  
368 the first 4 hours post-dosing.

369  
370  
371

**Discussion**

372

373

374 NEO212 is a hybrid molecule that was generated by conjugation of POH to TMZ. In all studies,  
375 NEO212 revealed stronger anticancer effects than its individual components, TMZ or POH by  
376 themselves, or the sum of its parts <sup>8,9,20,21</sup>. To further characterize the NEO212 molecule and  
377 understand its superior anticancer function, we now performed analytical measurements of its  
378 metabolism *in vitro* and *in vivo*.

379 Both TMZ and POH have undergone extensive clinical characterization in the past. Therefore,  
380 metabolic pathways for these two agents are very well established <sup>3,15</sup>. For NEO212, we  
381 hypothesized that esterase activity, which is abundantly present in biological systems, would  
382 hydrolyse the carbamate bond between the conjugated molecules to release POH and TMZ,  
383 which would then be subjected to the established metabolic processes. Based on results  
384 presented in the current report, this model indeed appears to be correct.

385

386 Using MS, we were able to identify NEO212, as well as its predicted key breakdown products  
387 TMZ and POH, in an aqueous solution (**Figure 1B**). AIC was identified also, which indirectly  
388 pointed to the generation of a methyl diazonium ion, which is the reactive species known to  
389 methylate DNA. MTIC, the intermediate between TMZ and AIC, was not detected, presumably  
390 due to its particularly short-lived nature. POH was readily identified by MS, although none of its  
391 metabolites. This was unsurprising, because POH requires specific enzymatic activities for  
392 stepwise oxidation to its metabolites PALD and PA, whereas in comparison the decay of TMZ to  
393 MTIC and AIC is a non-enzymatic process that spontaneously takes place in aqueous solution  
394 and neutral pH. It is noteworthy that the events of MS fragmentation take place in the presence  
395 of elevated energy molecular ions in a high vacuum, and therefore are not entirely reflective of  
396 solution chemistry of biological samples. For instance, breakage of the carbamide bond under  
397 MS conditions reflects its bombardment with electrons, as esterases were not present in the  
398 reaction conditions. This is also indicated by our detection of TMZ-carboxylic acid (TMZ-COOH)  
399 as a reaction species. Despite this limitation, MS analysis provided a preliminary portrait of  
400 NEO212 chemistry, which was further illuminated and complemented by HPLC-based analytical  
401 methods.

402

403 We employed published HPLC protocols <sup>16,31-33</sup> and successfully modified them toward the  
404 specific detection of NEO212, TMZ, POH, AIC, and PA from biological environments  
405 (**Supplementary Figure S1**), such as cell lysates, mouse plasma and brain tissue after

406 exposure to NEO212. In cell culture experiments, we established that the intracellular  
407 concentrations of TMZ and AIC were significantly higher in NEO212-treated cells than in TMZ-  
408 treated cells (**Figure 2**). Thus, despite identical drug concentrations in the culture medium,  
409 cellular uptake of NEO212 appears much more efficient than uptake of TMZ. Although we did  
410 not investigate details of the uptake mechanism, we deem it unlikely that this process involves  
411 prior extracellular decay of NEO212 into TMZ + POH, followed by POH-facilitated uptake of  
412 TMZ. This rationale is based on the fact that mere combination treatment of cells with individual  
413 components, i.e., TMZ mixed with POH, is unable to mimic the substantially greater cytotoxic  
414 potency of NEO212. Thus, the presence of POH in the extracellular space is not able to  
415 increase the cytotoxic potency of TMZ over that of TMZ alone, excluding a model based on  
416 efficient co-transport of two separate molecules into cells. Rather, in view of POH's amphipathic  
417 physiochemical character and its ability to intercalate into cellular membranes <sup>34</sup>, we propose  
418 that NEO212 efficiently associates with the membrane bilayer, where the conjugated TMZ  
419 moiety is towed along and eventually separated from the compound molecule by intracellular  
420 esterases. While validation of this conjecture remains to be established, the unequivocally  
421 greater presence of intracellular AIC after NEO212 treatment is reflective of increased delivery  
422 of DNA-alkylating, apoptosis-inducing methyldiazonium ions, thereby providing a straightforward  
423 explanation as to NEO212's greater cytotoxic potency over TMZ in cell culture.

424  
425 The treatment of all brain-localized diseases is limited by poor BBB penetration of most  
426 therapeutics. Even TMZ shows only partial ability to penetrate the BBB, with a brain-to-plasma  
427 ratio in the range of 10-25%, depending on the model used <sup>35,36</sup>. In our previous studies, we had  
428 used a computer program that predicted *in silico* whether a given compound would enter the  
429 BBB and exert activity in the brain <sup>18</sup>. By comparing NEO212 to TMZ, the program predicted  
430 superior performance by NEO212, which was further supported by results from *in vivo* studies,  
431 where we documented greater therapeutic impact of NEO212 as compared to TMZ in mouse  
432 brain tumor models <sup>8,9</sup>. The results shown in **Figure 3C** now provide analytic quantitation of this  
433 effect by revealing that brain:plasma ratios of NEO212 are 3-times higher than those of TMZ,  
434 after oral gavage of mice. This result points to favorable characteristics of NEO212 if used for  
435 brain malignancy. A recognized side effect of TMZ therapy is myelosuppression of the bone  
436 marrow, which limits dosing of this oral drug. Based on NEO212's alkylating properties,  
437 qualitative similar toxicities should be expected. However, based on the non-proliferative nature  
438 of brain cells, neurotoxicity should be low, and brain parenchyma should be able to tolerate  
439 increased drug dosages (as is the case with TMZ). Therefore, based on a 3-times increased

440 brain:plasma ratio, one would envision the possibility of delivering greater alkylating impact to  
441 the brain, while at the same time keeping systemic exposure (in particular bone marrow) at an  
442 equivalent level to TMZ. Therefore, at similar systemic toxicity as TMZ, NEO212 would be  
443 expected to achieve greater therapeutic impact on brain cancers. So far, the preclinical  
444 experience in mouse models is in agreement with this prediction, as these studies have  
445 documented superior activity of NEO212 in brain cancer, along with undetectable systemic  
446 toxicities. Furthermore, preferential uptake of NEO212 by brain tumor tissue over normal brain  
447 tissue, and respectively increased levels of AIC in brain tumors (as demonstrated in **Figure 4**),  
448 indicate additional features that bode well for future clinical applications. Moreover, its activity in  
449 MGMT-positive GB<sup>37</sup> cannot be overemphasized, as it may also be used to treat these patients  
450 who currently do not have much benefit from TMZ.

451  
452 Our study further establishes plasma half-life of NEO212 (94 minutes, **Figure 3**), which is only  
453 slightly longer than what has been reported for TMZ<sup>38</sup>. In view of repeat once-daily dosing, this  
454 fairly short half-life would not be expected to result in significant drug accumulation over time.  
455 Although this aspect will require further confirmation, the available data therefore suggest that a  
456 similar oral dosing schedule to TMZ would be appropriate in the clinical setting.

457  
458 In summary, our study introduces HPLC-based methods for quantification of NEO212 and  
459 several of its metabolites. We investigated *in vivo* metabolism of this novel conjugate and  
460 characterized the presence of TMZ, POH, AIC, and PA. The latter two are of particular interest,  
461 because they are longer-lived, easy to detect, and derived from the same initial molecule at  
462 stoichiometric ratios. As such, both AIC and PA represent suitable readouts for overall drug  
463 exposure. Their detection and quantification will support further studies on NEO212, and will  
464 become particularly useful during clinical trials, where drug exposure of patients requires careful  
465 characterization and monitoring.

466

**References**

467  
468  
469  
470  
471  
472  
473  
474  
475  
476  
477  
478  
479  
480  
481  
482  
483  
484  
485  
486  
487  
488  
489  
490  
491  
492  
493  
494  
495  
496  
497  
498  
499

1. Stupp R, Hegi ME, Mason WP, et al. Effects of radiotherapy with concomitant and adjuvant temozolomide versus radiotherapy alone on survival in glioblastoma in a randomised phase III study: 5-year analysis of the EORTC-NCIC trial. *Lancet Oncol.* 2009; 10(5):459-466.
2. Stupp R, Mason WP, van den Bent MJ, et al. Radiotherapy plus concomitant and adjuvant temozolomide for glioblastoma. *N Engl J Med.* 2005; 352(10):987-996.
3. Newlands ES, Stevens MF, Wedge SR, Wheelhouse RT, Brock C. Temozolomide: a review of its discovery, chemical properties, pre-clinical development and clinical trials. *Cancer Treat Rev.* 1997; 23(1):35-61.
4. Tsang LL, Farmer PB, Gescher A, Slack JA. Characterisation of urinary metabolites of temozolomide in humans and mice and evaluation of their cytotoxicity. *Cancer Chemother Pharmacol.* 1990; 26(6):429-436.
5. Fahrner J, Kaina B. O6-methylguanine-DNA methyltransferase in the defense against N-nitroso compounds and colorectal cancer. *Carcinogenesis.* 2013; 34(11):2435-2442.
6. Fu D, Calvo JA, Samson LD. Balancing repair and tolerance of DNA damage caused by alkylating agents. *Nat Rev Cancer.* 2012; 12(2):104-120.
7. Weller M, Cloughesy T, Perry JR, Wick W. Standards of care for treatment of recurrent glioblastoma--are we there yet? *Neuro Oncol.* 2013; 15(1):4-27.
8. Chen TC, Cho HY, Wang W, et al. A novel temozolomide-perillyl alcohol conjugate exhibits superior activity against breast cancer cells in vitro and intracranial triple-negative tumor growth in vivo. *Mol Cancer Ther.* 2014; 13(5):1181-1193.
9. Cho HY, Wang W, Jhaveri N, et al. NEO212, temozolomide conjugated to perillyl alcohol, is a novel drug for effective treatment of a broad range of temozolomide-resistant gliomas. *Mol Cancer Ther.* 2014; 13(8):2004-2017.
10. Chen TC, Fonseca CO, Schonthal AH. Preclinical development and clinical use of perillyl alcohol for chemoprevention and cancer therapy. *Am J Cancer Res.* 2015; 5(5):1580-1593.
11. Cho HY, Wang W, Jhaveri N, et al. Perillyl alcohol for the treatment of temozolomide-resistant gliomas. *Mol Cancer Ther.* 2012; 11(11):2462-2472.
12. Sundin T, Peffley DM, Gauthier D, Hentosh P. The isoprenoid perillyl alcohol inhibits telomerase activity in prostate cancer cells. *Biochimie.* 2012; 94(12):2639-2648.

- 500 **13.** da Fonseca CO, Schwartzmann G, Fischer J, et al. Preliminary results from a phase I/II  
501 study of perillyl alcohol intranasal administration in adults with recurrent malignant  
502 gliomas. *Surg Neurol.* 2008; 70(3):259-266; discussion 266-257.
- 503 **14.** da Fonseca CO, Simao M, Lins IR, Caetano RO, Futuro D, Quirico-Santos T. Efficacy of  
504 monoterpene perillyl alcohol upon survival rate of patients with recurrent glioblastoma. *J*  
505 *Cancer Res Clin Oncol.* 2011; 137(2):287-293.
- 506 **15.** Phillips LR, Malspeis L, Supko JG. Pharmacokinetics of active drug metabolites after  
507 oral administration of perillyl alcohol, an investigational antineoplastic agent, to the dog.  
508 *Drug Metab Dispos.* 1995; 23(7):676-680.
- 509 **16.** Hua HY, Zhao YX, Liu L, Ye QX, Ge SW. High-performance liquid chromatographic and  
510 pharmacokinetic analyses of an intravenous submicron emulsion of perillyl alcohol in  
511 rats. *J Pharm Biomed Anal.* 2008; 48(4):1201-1205.
- 512 **17.** Ripple GH, Gould MN, Stewart JA, et al. Phase I clinical trial of perillyl alcohol  
513 administered daily. *Clin Cancer Res.* 1998; 4(5):1159-1164.
- 514 **18.** Chen TC, Da Fonseca CO, Schonthal AH. Perillyl Alcohol and Its Drug-Conjugated  
515 Derivatives as Potential Novel Methods of Treating Brain Metastases. *Int J Mol Sci.*  
516 2016; 17(9).
- 517 **19.** Jhaveri N, Agasse F, Armstrong D, et al. A novel drug conjugate, NEO212, targeting  
518 proneural and mesenchymal subtypes of patient-derived glioma cancer stem cells.  
519 *Cancer Lett.* 2016; 371(2):240-250.
- 520 **20.** Chen TC, Cho HY, Wang W, et al. A novel temozolomide analog, NEO212, with  
521 enhanced activity against MGMT-positive melanoma in vitro and in vivo. *Cancer Lett.*  
522 2015; 358(2):144-151.
- 523 **21.** Chen TC, Cho HY, Wang W, et al. Chemotherapeutic effect of a novel temozolomide  
524 analog on nasopharyngeal carcinoma in vitro and in vivo. *J Biomed Sci.* 2015; 22:71.
- 525 **22.** Xie L, Song X, Guo W, et al. Therapeutic effect of TMZ-POH on human nasopharyngeal  
526 carcinoma depends on reactive oxygen species accumulation. *Oncotarget.* 2016;  
527 7(2):1651-1662.
- 528 **23.** Song X, Liu L, Chang M, et al. NEO212 induces mitochondrial apoptosis and impairs  
529 autophagy flux in ovarian cancer. *J Exp Clin Cancer Res.* 2019; 38(1):239.
- 530 **24.** Chang M, Song X, Geng X, et al. Temozolomide-Perillyl alcohol conjugate impairs  
531 Mitophagy flux by inducing lysosomal dysfunction in non-small cell lung Cancer cells and  
532 sensitizes them to irradiation. *J Exp Clin Cancer Res.* 2018; 37(1):250.

- 533 **25.** Song X, Xie L, Chang M, et al. Temozolomide-perillyl alcohol conjugate downregulates  
534 O(6)-methylguanin DNA methltransferase via inducing ubiquitination-dependent  
535 proteolysis in non-small cell lung cancer. *Cell Death Dis.* 2018; 9(2):202.
- 536 **26.** Song X, Xie L, Wang X, et al. Temozolomide-perillyl alcohol conjugate induced reactive  
537 oxygen species accumulation contributes to its cytotoxicity against non-small cell lung  
538 cancer. *Sci Rep.* 2016; 6:22762.
- 539 **27.** Silva-Hirschberg C, Hartman H, Stack S, et al. Cytotoxic impact of a perillyl alcohol-  
540 temozolomide conjugate, NEO212, on cutaneous T-cell lymphoma in vitro. *Ther Adv*  
541 *Med Oncol.* 2019; 11:1758835919891567.
- 542 **28.** Cho HY, Thein TZ, Wang W, et al. The Rolipram-Perillyl Alcohol Conjugate (NEO214) Is  
543 A Mediator of Cell Death through the Death Receptor Pathway. *Mol Cancer Ther.* 2019;  
544 18(3):517-530.
- 545 **29.** Elegbede JA, Flores R, Wang RC. Perillyl alcohol and perillaldehyde induced cell cycle  
546 arrest and cell death in BroTo and A549 cells cultured in vitro. *Life Sci.* 2003;  
547 73(22):2831-2840.
- 548 **30.** Yeruva L, Pierre KJ, Elegbede A, Wang RC, Carper SW. Perillyl alcohol and perillic acid  
549 induced cell cycle arrest and apoptosis in non small cell lung cancer cells. *Cancer Lett.*  
550 2007; 257(2):216-226.
- 551 **31.** de Lima DC, Rodrigues SV, Boaventura GT, et al. Simultaneous measurement of perillyl  
552 alcohol and its metabolite perillic acid in plasma and lung after inhalational  
553 administration in Wistar rats. *Drug Test Anal.* 2020; 12(2):268-279.
- 554 **32.** Kim H, Likhari P, Parker D, et al. High-performance liquid chromatographic analysis and  
555 stability of anti-tumor agent temozolomide in human plasma. *J Pharm Biomed Anal.*  
556 2001; 24(3):461-468.
- 557 **33.** Shen F, Decosterd LA, Gander M, Leyvraz S, Biollax J, Lejeune F. Determination of  
558 temozolomide in human plasma and urine by high-performance liquid chromatography  
559 after solid-phase extraction. *J Chromatogr B Biomed Appl.* 1995; 667(2):291-300.
- 560 **34.** da Fonseca CO, Khandelia H, Salazar MD, Schonthal AH, Meireles OC, Quirico-Santos  
561 T. Perillyl alcohol: Dynamic interactions with the lipid bilayer and implications for long-  
562 term inhalational chemotherapy for gliomas. *Surg Neurol Int.* 2016; 7:1.
- 563 **35.** Ostermann S, Csajka C, Buclin T, et al. Plasma and cerebrospinal fluid population  
564 pharmacokinetics of temozolomide in malignant glioma patients. *Clin Cancer Res.* 2004;  
565 10(11):3728-3736.

- 566 **36.** Portnow J, Badie B, Chen M, Liu A, Blanchard S, Synold TW. The  
567 neuropharmacokinetics of temozolomide in patients with resectable brain tumors:  
568 potential implications for the current approach to chemoradiation. *Clin Cancer Res.*  
569 2009; 15(22):7092-7098.
- 570 **37.** Marin-Ramos NI, Thein TZ, Cho HY, et al. NEO212 Inhibits Migration and Invasion of  
571 Glioma Stem Cells. *Mol Cancer Ther.* 2018; 17(3):625-637.
- 572 **38.** Reyderman L, Statkevich P, Thonoor CM, Patrick J, Batra VK, Wirth M. Disposition and  
573 pharmacokinetics of temozolomide in rat. *Xenobiotica.* 2004; 34(5):487-500.

574

575

576 **Figure Captions:**

577

578 **Figure 1. The chemical structure and predicted breakdown products of NEO212**

579 (A) NEO212 is a conjugation product of POH and TMZ, where the two components are  
580 connected *via* a carbamate bridge. NEO212 might decay into POH and TMZ. The  
581 methyl diazonium ion alkylates O<sup>6</sup>MeG DNA lesions and triggers apoptosis. POH and PA  
582 contribute to tumor cell death *via* aggravation of ER stress. (B) NEO212 breakdown product  
583 analysis using MS.

584

585 **Figure 2. Cellular uptake of NEO212 compared to TMZ**

586 U251TR cells were treated with 100  $\mu$ M of either NEO212 or TMZ. (A) The amount of  
587 intracellular TMZ was measured using MS. (B) The amount of intracellular AIC was measured  
588 using MS. All differences were statistically significant. (C) Colony forming assay was performed  
589 using different concentrations of drugs using U251TR cells.

590

591 **Figure 3. Half-life of NEO212 or AIC in mouse plasma**

592 (A) NEO212 concentrations were measured in plasma by HPLC after oral administration (left) or  
593 subcutaneous administration (right) of NEO212 (50 mg/kg) to C57BL/6 mice. (B) AIC  
594 concentrations in plasma were measured using HPLC after administration of NEO212 (50  
595 mg/kg) or TMZ (50 mg/kg) to C57BL/6 mice. The concentrations for each sample were  
596 converted from the area under the curve (AUC) for the AIC peak detected. (C) Brain:plasma  
597 ratio of NEO212 and TMZ. Two asterisks (\*\*):  $p < 0.015$ .

598

599 **Figure 4. Differential uptake of NEO212 or AIC in normal and tumor-bearing brains.**

600 (A) NEO212 concentrations in the tumor-bearing brain and normal brain (\*\*:  $p < 0.015$ ). (B) AIC  
601 concentrations in the tumor-bearing brain and normal brain (\*\*:  $p < 0.001$ ). (C) Overall

602 comparison of brain to plasma ratios of NEO212 ( $p < 0.015$ ). (D) POH concentrations in the  
603 tumor-bearing brain and normal brain (\*\*:  $p < 0.015$ ). (E) PA concentrations in the tumor-bearing  
604 brain and normal brain (\*\*:  $p < 0.001$ ).

605

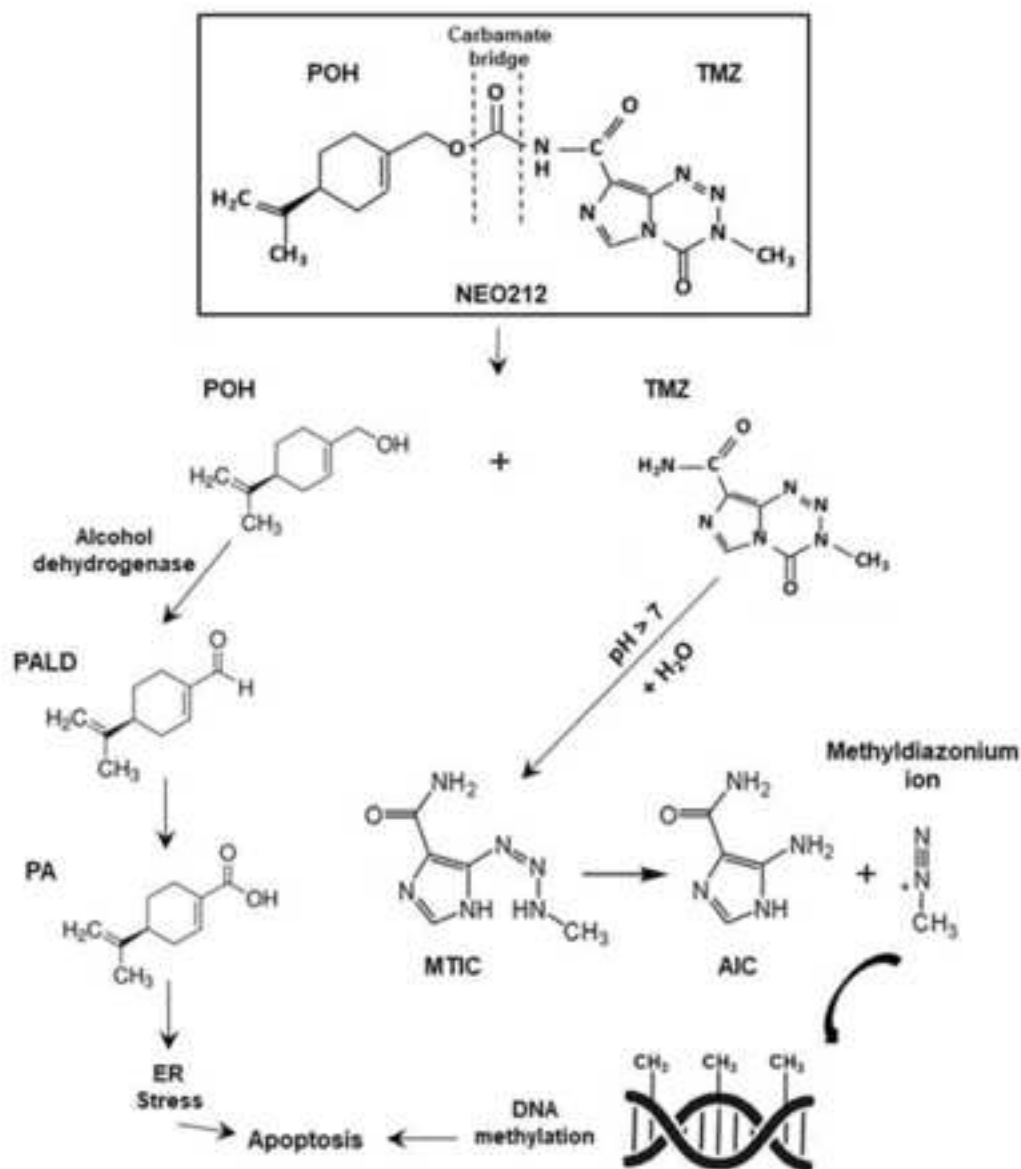
606 **Figure 5. Excretion of NEO212 with oral administration.**

607 (A) Time profile of NEO212 in urine and feces. (B) Time profile of AIC in urine and feces.

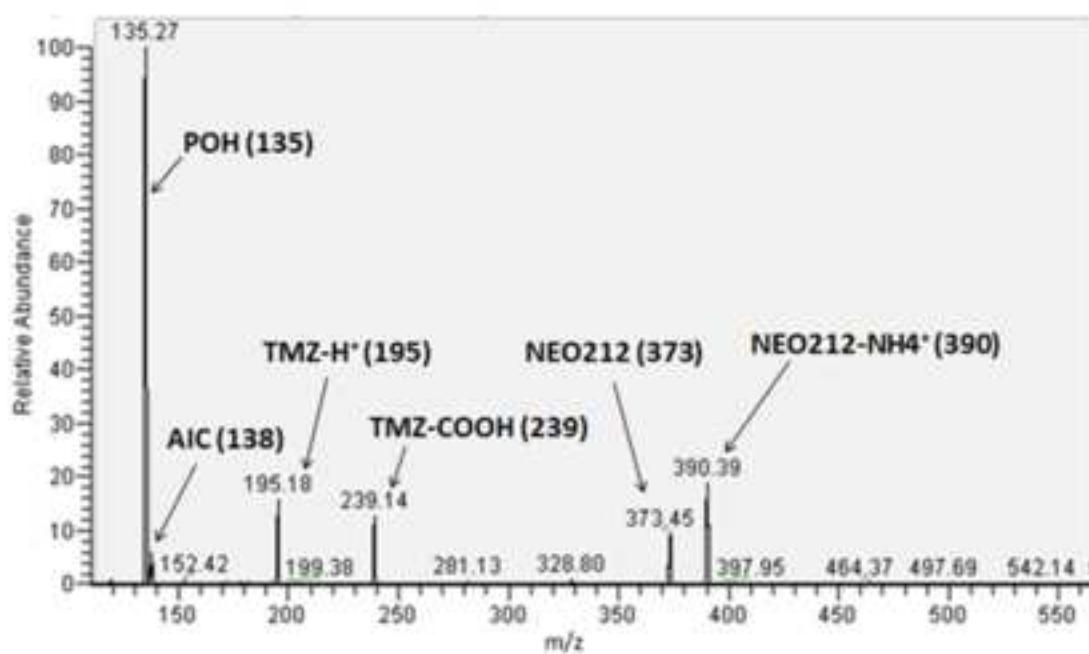
608

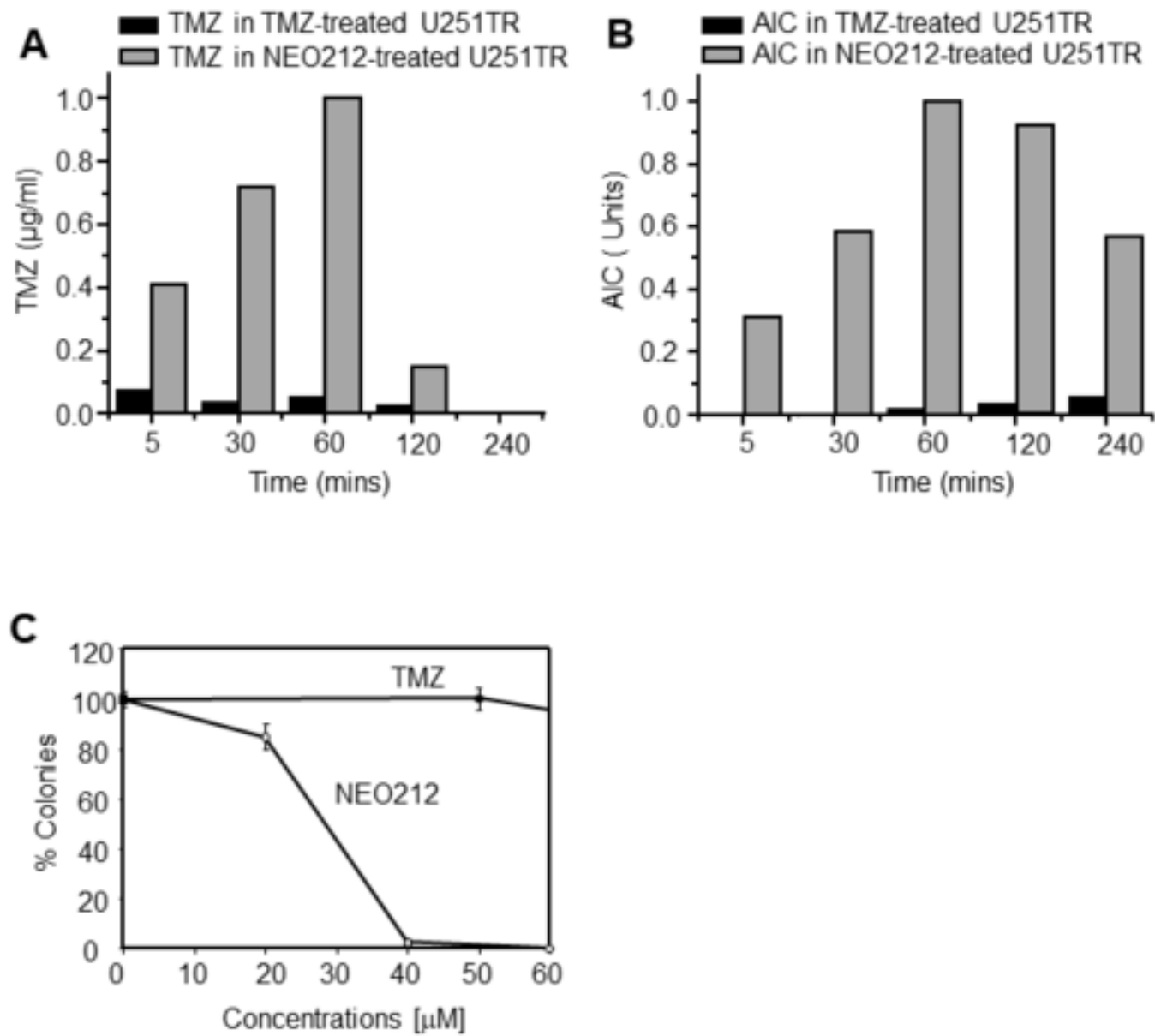
Figure 1

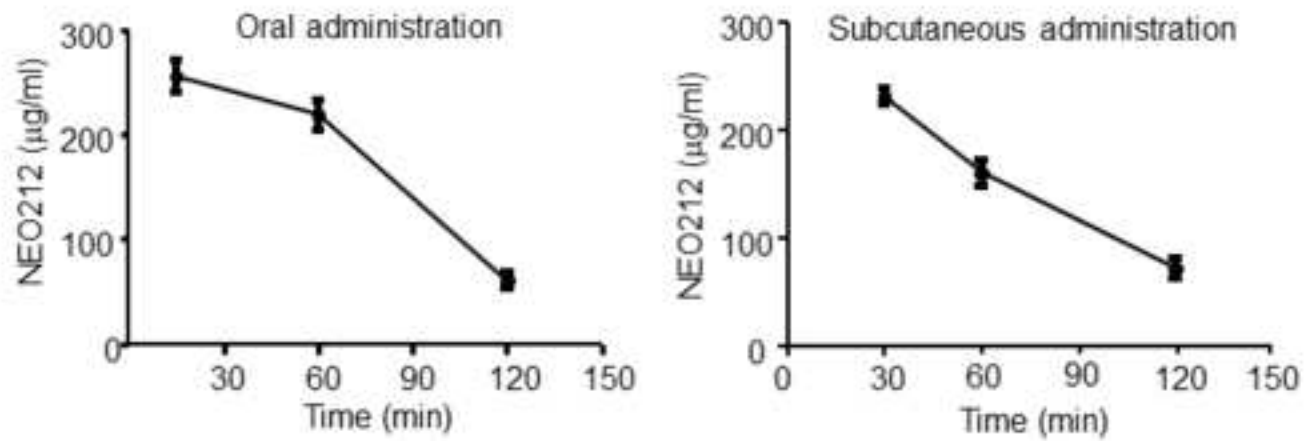
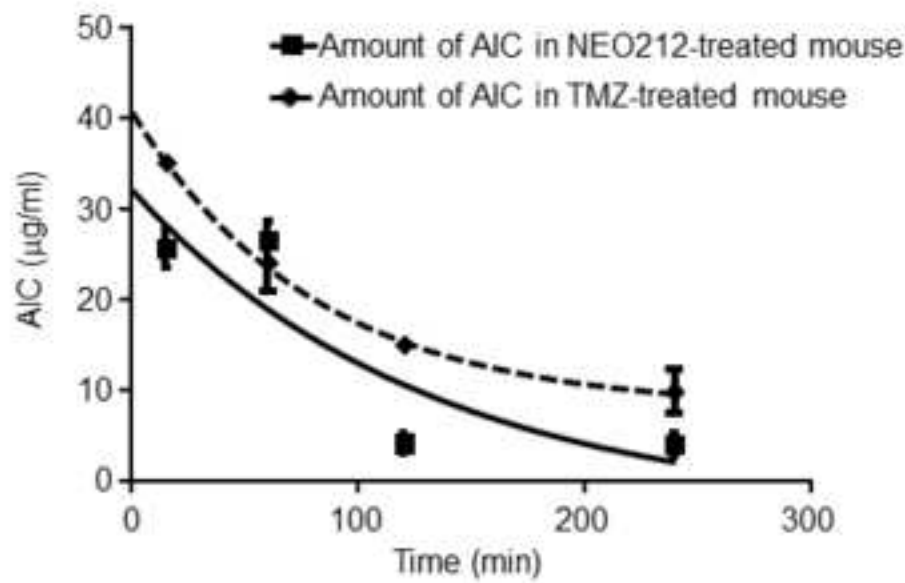
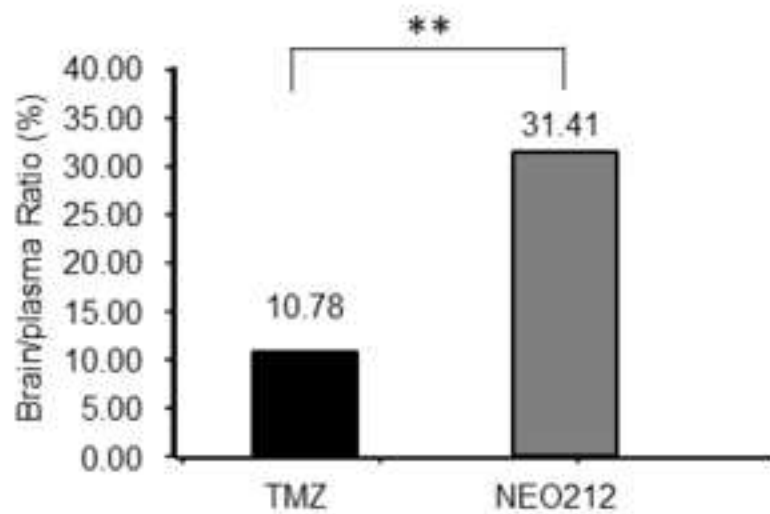
A

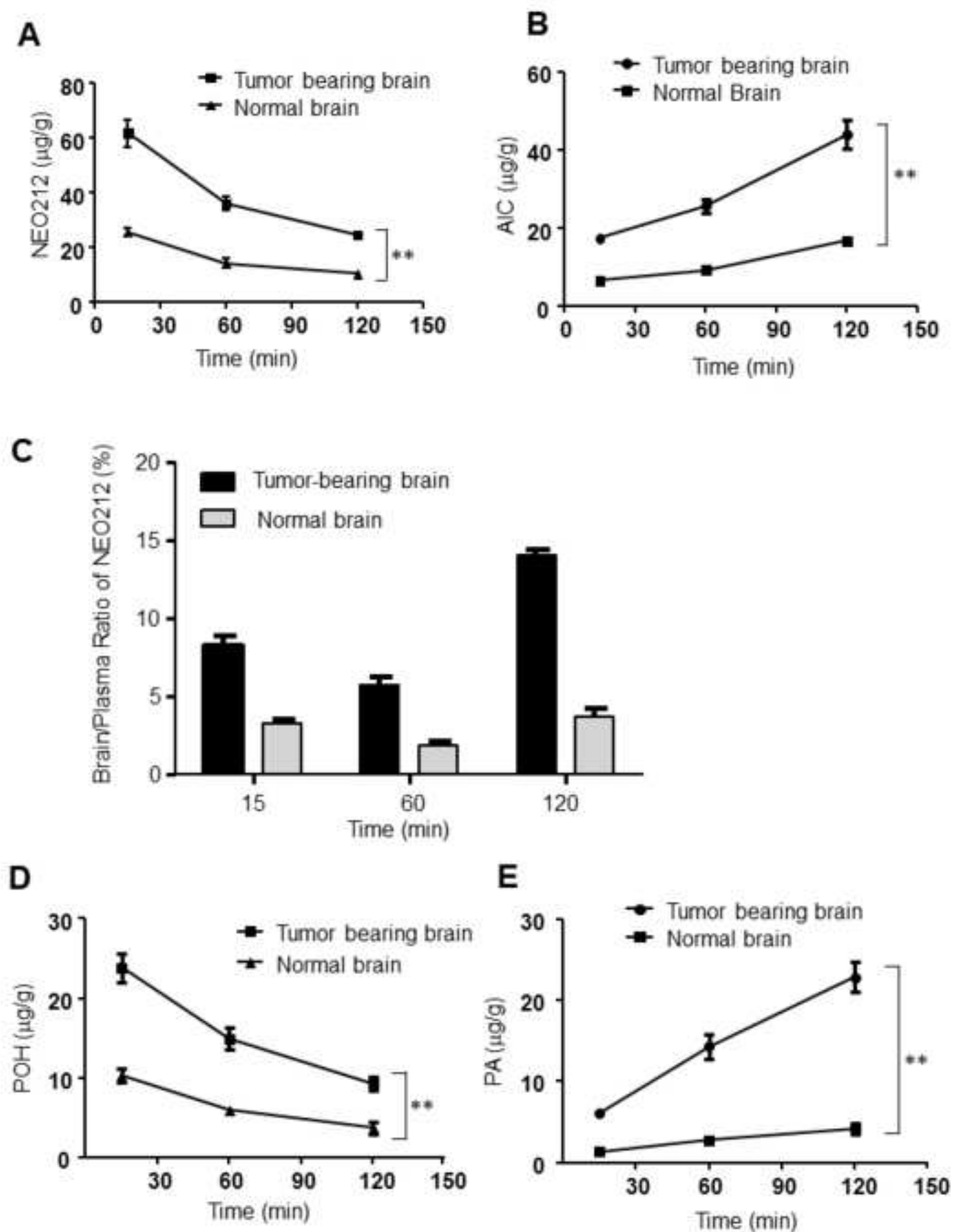


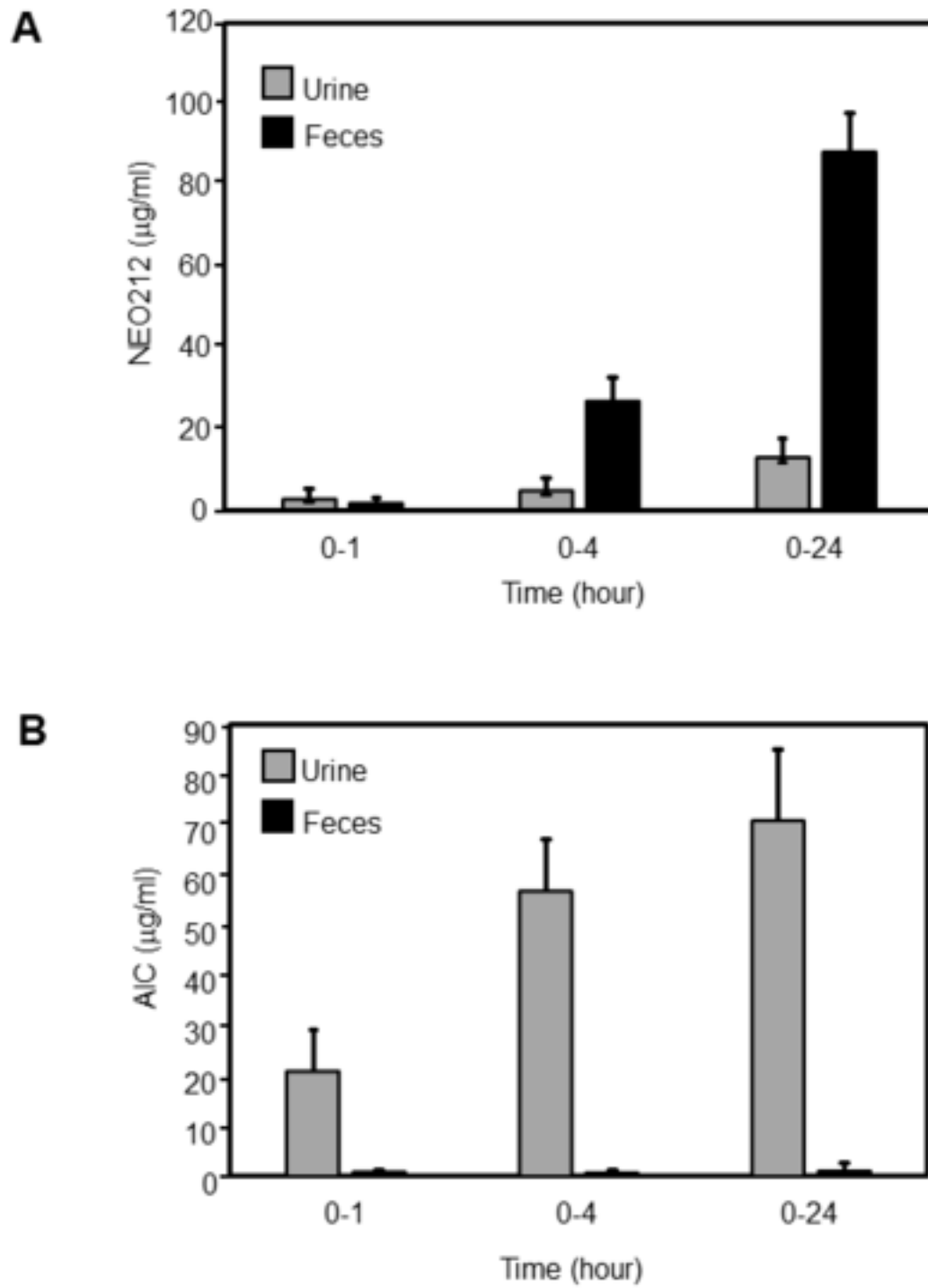
B



**Figure 2**

**Figure 3****A****B****C**

**Figure 4**

**Figure 5**



## **SUPPLEMENTARY METHODS**

### **Cell culture**

The human glioma cell lines LN229, T98G, U251, and U251TR, as well as the mouse glioma cell line GL261, were propagated in Dulbecco's Modified Eagle Medium (DMEM) supplemented with 10% fetal bovine serum (FBS), 100 U/mL penicillin, and 0.1 mg/mL streptomycin in a humidified incubator at 37°C and a 5% CO<sub>2</sub> atmosphere. USC02 glioma cancer stem cells were cultured in cancer stem cell culture (CSC) medium containing DMEM-F12 medium (Life Technologies, Grand Island, NY) with 1% penicillin-streptomycin, 1% B-27 (Life Technologies), 20 ng/ml EGF and FGF-2 (Peprotech, Rocky Hill, NJ).

### **Colony Forming Assay (CFA)**

Glioma cells were seeded in 6-well plates at 200 cells/ well and allowed to adhere overnight. Subsequently, cells were treated with drugs for 48 hours; the medium was then removed and fresh medium (without drug) was added. Cells were incubated for an additional 7-10 days. At the termination of the assay, colonies were visualized by staining with 1% methylene blue in methanol for 4 hours. Dyes were washed out with water and then air dried. The stained colonies were counted. Percent colonies were calculated relative to untreated control cells. All experiments were performed in triplicate. Vehicle-treated cells were also included, but showed no difference to untreated cells.

### **MTT cytotoxicity assay**

Glioma stem cells (GSCs) were seeded in 96 well plates in CSC medium containing BSA (Sigma Aldrich) equivalent to 10% FCS. After 24 hours, TMZ or NEO212 was added to the cells at different concentrations, and incubated for 72 hours. The MTT assay was performed according to the manufacturer's protocol (Sigma Aldrich, St. Louis, MO). Absorbance was measured using a microtiter plate reader (Molecular Devices, Sunnyvale, CA) at 490 nm. Percent viability was calculated relative to untreated control cells. All experiments were performed in triplicate.

### **Bioassay of NEO212 and its metabolites by mass spectrometry (MS)**

Cell lysates were stabilized with 100 mM ammonium acetate (AmAc) (pH 4.0), followed by a simple protein precipitation method with methanol to clean up the samples prior to analysis. After vortexing for 15 sec, the solutions were chilled at -20°C for 20 min and centrifuged at 4°C

54 using 20817 xg for 20 min. The supernatant was directly injected into the MS instrument for  
55 analysis. Calibration curves for each drug were generated for quantification. Individual stock  
56 solutions of TMZ (400 µg/ml) (Sigma Aldrich), NEO212 (400 µg/ml) and angiotensin II (40 µg/ml;  
57 internal standard) were serially diluted with acidic methanol (methanol:1M AmAc = 90:10).

58

### 59 **HPLC Analysis**

60 All plasma or brain lysate samples (100 µl) were mixed with 200 µl acetonitrile and filtered with  
61 a 0.22 µm nylon filter (Nalgene) or a 4k MW cut-off filter. A 10-µl aliquot of filtrate was injected  
62 into an i-Series Plus Integrated HPLC System (Shimadzu, Columbia, MD) with an integrated  
63 photo-diode array detector (PDA). LabSolutions V5.87 SP1 software (Shimadzu) was used for  
64 data acquisition and instrument control. The isocratic separation of NEO212, TMZ, POH and PA  
65 was performed using a Roc C18 column (10 x 4.6 mm x 3 µm) (Restek Corporation, Bellefonte,  
66 PA) with a column temperature of 30°C for 30 minutes. The mobile phase consisted of  
67 acetonitrile plus 0.1% trifluoroacetic acid (TFA): water plus 0.1% TFA (pH 4.0) (40:60 v/v). The  
68 AIC gradient separation utilized A (water-acetonitrile-trichloroacetic acid, 95:5:0.1, v/v/v) and B  
69 (water-acetonitrile-trichloroacetic acid, 5:95:0.1, v/v/v) 100% A to 100% B. Flow rate was 1.0  
70 mL/min with a temperature of 30°C. As internal standard, ibuprofen (Cayman Chemical, Ann  
71 Arbor, MI) was utilized.

72

### 73 **Plasma sample preparation**

74 Mice were euthanized and 300 µl of blood was collected and acidified by addition of 300 µl of  
75 citrate buffer (0.8% sodium citrate in H<sub>2</sub>O). The tube was gently inverted 8-10 times until  
76 thoroughly mixed. The samples were placed on ice and centrifuged at 4°C within 30 minutes. All  
77 samples were prepared in triplicate.

78

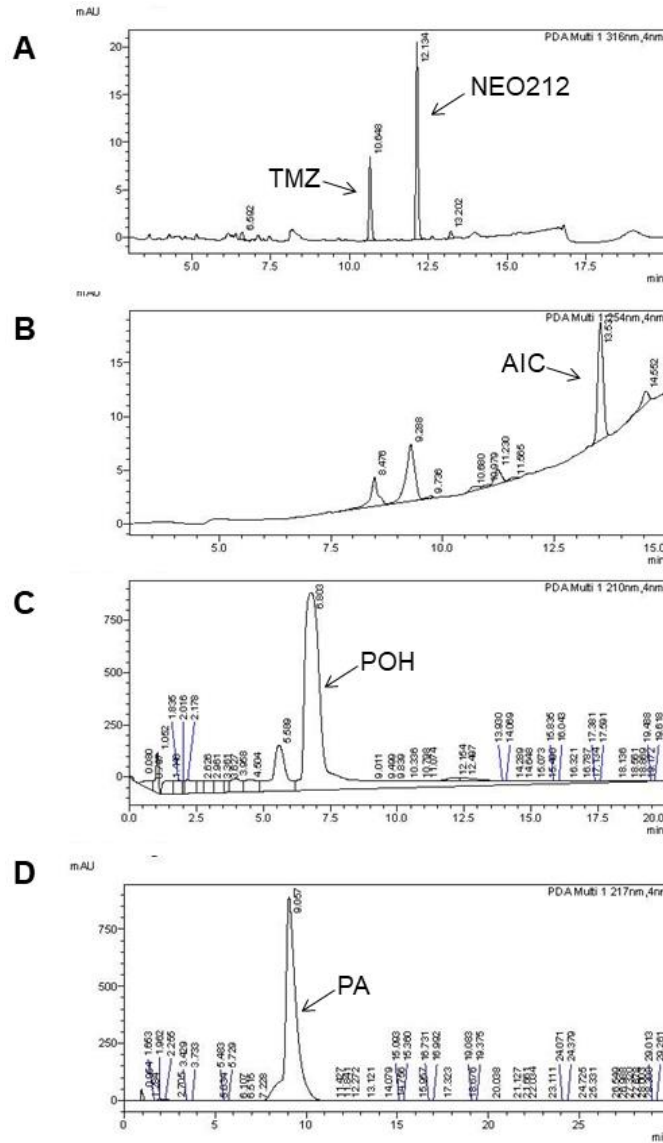
### 79 **Brain tissue homogenate preparation**

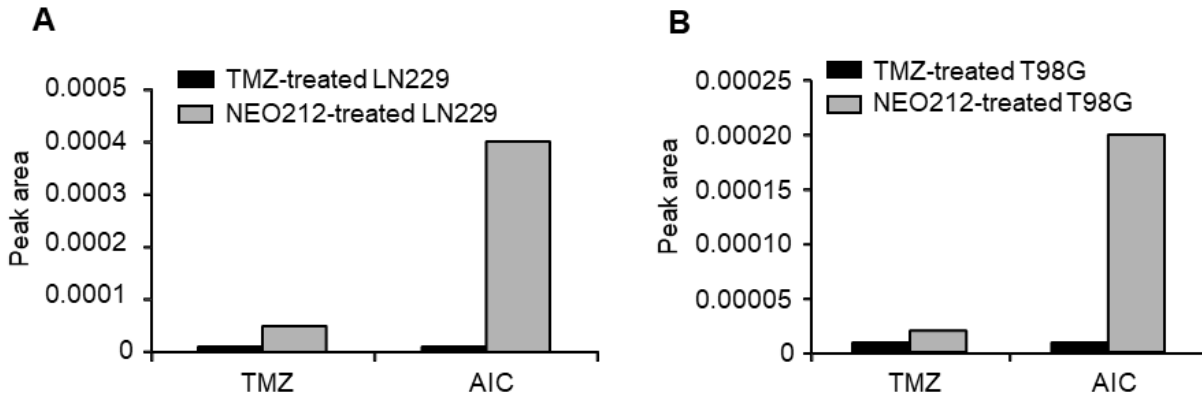
80 Mouse brain was washed once with ice-cold PBS and homogenized in 1 ml of ammonium  
81 acetate buffer (pH 4.0) in a tissue homogenizer. The lysate was centrifuged at 12,000 rpm for  
82 15 minutes. The supernatant was collected and stored at -80°C until analyzed by HPLC. All  
83 samples were prepared in triplicate.

84

85 **SUPPLEMENTARY FIGURES**

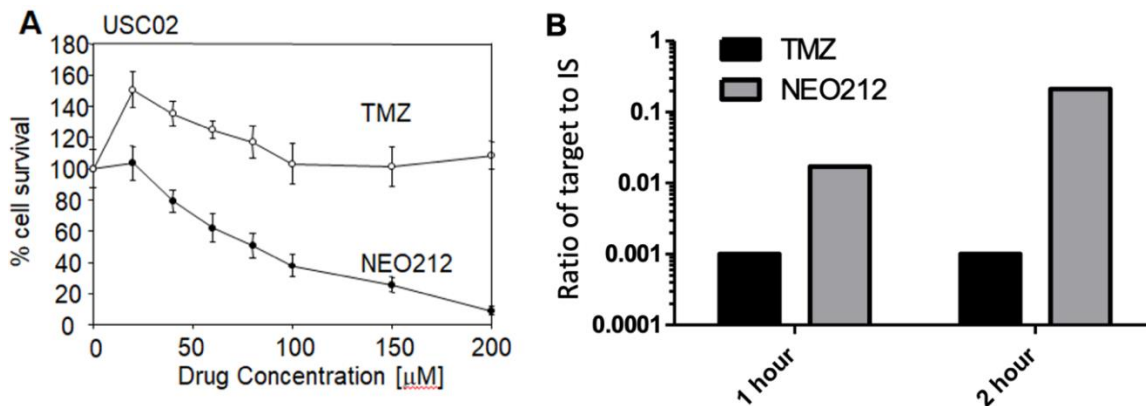
86  
87  
88  
89





96  
97  
98 **Supplementary Figure S2. Cellular uptake of NEO212 compared to TMZ in LN229 and T98G glioma cell lines**

99 (A) The amount of intracellular TMZ or AIC in LN229 cells at 60 minutes after treatment with 100  
100  $\mu\text{M}$  of either NEO212 or TMZ was measured by mass spectroscopy (MS). (B) The amount of  
101 intracellular TMZ or AIC in T98G cells at 60 minutes after treatment with 100  $\mu\text{M}$  of either  
102 NEO212 or TMZ was measured by MS. All differences between TMZ-treated cells and  
103 NEO212-treated cells were statistically significant ( $p < 0.05$ ).



108  
109  
110 **Supplementary Figure S3. Cytotoxicity and cellular uptake of TMZ and NEO212 in chemoresistant glioma cancer stem cells USC02**

111 USC02 is highly drug-resistant glioma stem cell line isolated from a patient with glioblastoma. (A)  
112 MTT cytotoxicity assay with TMZ (white circles) or NEO212 (black circles) using MTT assay in  
113 USC02. As shown, NEO212 began to exert cytotoxic activity at concentrations below 50  $\mu\text{M}$   
114 ( $p < 0.05$ ), whereas TMZ was not toxic at 200  $\mu\text{M}$ . Data are expressed as percent cell survival  
115 relative to untreated control. All conditions were performed in triplicate. (B) The amount of  
116 intracellular TMZ or NEO212 at 1 and 2 hours after treatment of USC02 cells with 100  $\mu\text{M}$  TMZ  
117 or NEO212, as measured using MS. Shown is the relative amount of each compound (target) as  
118 a ratio to internal standard (IS). Difference between TMZ and NEO212 was significant ( $p < 0.001$ ).